Predicting and verifying transition strengths from weakly bound molecules

K. Aikawa,[1,*] D. Akamatsu,[2,†] M. Hayashi,[1,‡] J. Kobayashi,[2] M. Ueda,[3,4] and S. Inouye[2,3]

[1] *Department of Applied Physics, The University of Tokyo, Hongo, Bunkyo-ku, Tokyo 113-8656, Japan*
[2] *Institute of Engineering Innovation, The University of Tokyo, Yayoi, Bunkyo-ku, Tokyo 113-8656, Japan*
[3] *JST, ERATO, Yayoi, Bunkyo-ku, Tokyo 113-8656, Japan*
[4] *Department of Physics, The University of Tokyo, Hongo, Bunkyo-ku, Tokyo 113-0033, Japan*

(Dated: November 8, 2010)

We investigated transition strengths from ultracold weakly bound $^{41}K^{87}Rb$ molecules produced via the photoassociation of laser-cooled atoms. An accurate potential energy curve of the excited state $(3)^1\Sigma^+$ was constructed by carrying out direct potential fit analysis of rotational spectra obtained via depletion spectroscopy. Vibrational energies and rotational constants extracted from the depletion spectra of v' =41–50 levels were combined with the results of the previous spectroscopic study, and they were used for modifying an *ab initio* potential. An accuracy of 0.14% in vibrational level spacing and 0.3% in rotational constants was sufficient to predict the large observed variation in transition strengths among the vibrational levels. Our results show that transition strengths from weakly bound molecules are a good measure of the accuracy of an excited state potential.

PACS numbers: 34.20.-b,33.15.Bh,37.10.Mn,82.80.Ms

I. INTRODUCTION

Ultracold molecular gas is a prominent candidate for realizing novel distinctive applications in physics and chemistry, including precision measurements, quantum computation, ultracold chemistry, and novel quantum phases [1, 2]. Thus far the production of ultracold molecules in the vibrational ground state has been dependent on the optical transfer of weakly bound molecules formed via either photoassociation [3] or magnetoassociation [4]. Among the previously proposed methods [5–10], stimulated Raman adiabatic passage (STIRAP) [11–13] of weakly bound molecules is the most efficient method for preparing a molecular sample in a single quantum state.

In the STIRAP transfer, an excited state is used as an intermediate state. It is important to select an excited state having large transition strengths from both weakly bound and deeply bound levels. In general, the strengths of molecular transitions from low vibrational levels are readily predicted on the basis of the Franck-Condon factors (FCFs) calculated from a potential energy curve or molecular constants [14]. The small number of nodes in the radial wavefunction for a low vibrational level indicates a low sensitivity to deviations in the radial direction, thereby enabling us to explain the intensity distribution over vibrational levels from molecular constants. However, it is difficult to predict transition strengths from weakly bound molecular levels because weakly bound levels have a large number of nodes in their wavefunctions; hence, the FCFs are quite sensitive to the wavefunctions of excited states. In this letter, we show that transition strengths from weakly bound levels can be predicted on the basis of an accurate potential energy curve of the excited state, constructed via direct potential fit (DPF) analysis [15] of both vibrational energies and rotational constants.

We focused on the $(3)^1\Sigma^+$ state of KRb in the range

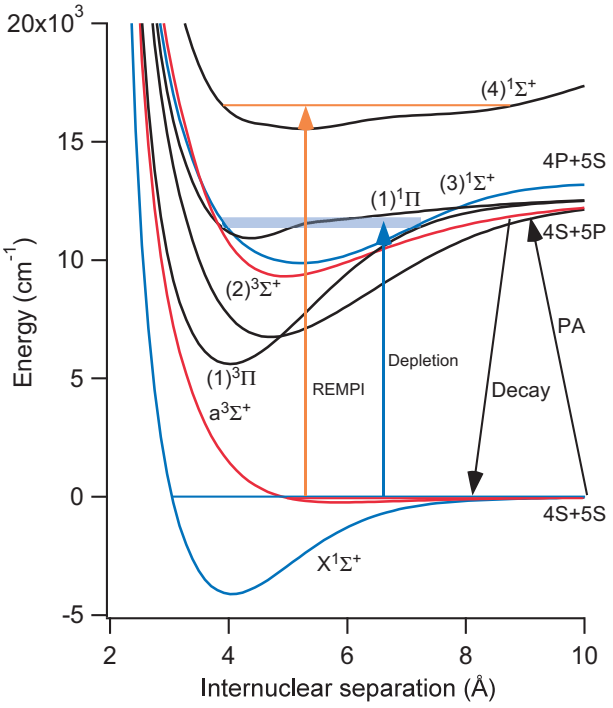

FIG. 1. Relevant potential energy curves of KRb. Weakly bound molecules were produced by the photoassociation of laser-cooled ^{41}K and ^{87}Rb atoms. The $(3)^1\Sigma^+$ state was investigated via the spectroscopy of molecules in the $v'' = 91$ level of $X^1\Sigma^+$. The intermediate state for REMPI ionization was the $(4)^1\Sigma^+$ state.

* ka_cypridina@atomtrap.t.u-tokyo.ac.jp
† Present address: National Metrology Institute of Japan, Tsukuba 305-8563, Japan
‡ Present address: NIKON CORPORATION, Kanagawa 252-0328, Japan

11400–11800 cm^{-1} with respect to the ground atomic threshold, which was proposed as a potential candidate for the STIRAP transfer of weakly bound molecules to the rovibrational ground state [16]. An RKR potential curve of the $(3)^1\Sigma^+$ state was reported from the potential minimum up to 10400 cm^{-1} [17]. An ionization spectrum for ^{39}K^{87}Rb obtained by using a pulse laser and a depletion spectrum near 11700 cm^{-1} is provided in Ref. 16. Recently, we have realized the STIRAP transfer of weakly bound molecules ($v'' = 91$, $J'' = 0$ of $X^1\Sigma^+$) to the rovibrational ground state ($v'' = 0$, $J'' = 0$ of $X^1\Sigma^+$), mediated by the $v' = 41$ level of the $(3)^1\Sigma^+$ state [18]. Before conducting this experiment, we carried out depletion spectroscopy in the range 11400–11800 cm^{-1}, which revealed 10 vibrational levels. We found that the width of the observed spectra was highly dependent on the vibrational levels of the $(3)^1\Sigma^+$ state. By introducing an analytical representation for power broadening, we extracted the transition strengths for each vibrational level. The other electronic states that correlate with the $(3)^1\Sigma^+$ state via spin-orbit interaction were far away; hence we assumed that most of the perturbations from these electronic states were negligible. Thus, we could analyze the experimentally obtained spectra on the basis of a single potential curve. In addition to the previous spectroscopic work near the bottom of the potential [17], vibrational energies and rotational constants extracted from the spectra were used to construct an accurate potential via DPF analysis. Using the modified potential, it was possible to explain the variation in transition strengths among the vibrational levels of the $(3)^1\Sigma^+$ state in terms of the FCFs.

II. DEPLETION SPECTROSCOPY

Previously, our experimental setup for the spectroscopy of ultracold ^{41}K^{87}Rb molecules was described in detail [19]. We provide a brief summary herein. We started with a dual-species magneto-optical trap (MOT) of 1×10^8 ^{41}K atoms and 2×10^8 ^{87}Rb atoms. A compressed MOT (C-MOT) procedure was applied for 40 ms to compress and cool the ^{41}K and ^{87}Rb atoms. The typical densities and temperatures of ^{41}K and ^{87}Rb at the end of C-MOT were 2×10^{11} cm^{-3} and 400 μK and 4×10^{11} cm^{-3} and 100 μK for ^{87}Rb, respectively. A photoassociation (PA) laser (wavenumber, 12570.13 cm^{-1}; intensity, 1×10^3 Wcm^{-2}) was applied for 10 ms at the end of the C-MOT process. The produced molecules were detected using micro-channel plates (MCP) after they were ionized via resonance enhanced multi-photon ionization (REMPI) using a pulsed dye laser (wavenumber, 16543 cm^{-1}; intensity, 3×10^6 W cm^{-2}).

Depletion spectra were obtained by monitoring ion counts in the $v'' = 91$ level of $X^1\Sigma^+$, while a CW Ti:Sapphire laser (Sirah Matisse TX; intensity, 50 Wcm^{-2}; beam waist, 350 μm) was continuously applied and scanned. In the present study, we analyzed spectra for the $v'' = 91$, $J'' = 2$ level, whose binding energy with respect to the atomic threshold $F_{\rm K}$=1+$F_{\rm Rb}$=1 was measured as $-12.454(1)$ cm^{-1}. The frequency of the Ti:Sapphire laser was monitored using a Fabry-Perot cavity which was locked to ^{87}Rb D2 line. The cavity transmission signal was used to calibrate the variation in the scanning speed and to measure the relative frequency of the laser with respect to the cavity transmission peak with a precision of 3 MHz. The absolute frequency was measured using a commercial wavemeter (Wavelength WS-7; accuracy, 60 MHz). The accuracy of measurements for rotational constants was limited by the spectral width, which was of the order of 100 MHz, whereas that for vibrational energies was limited by both the spectral width and the wavemeter.

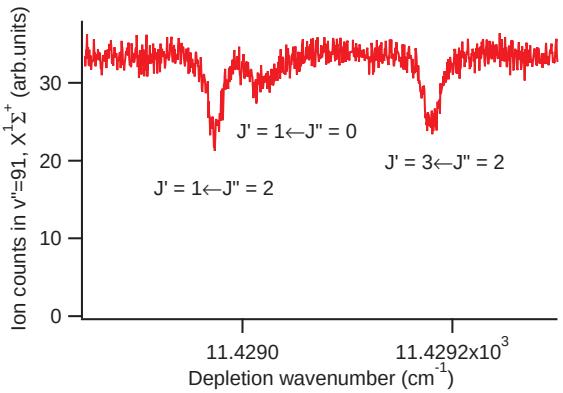

FIG. 2. Depletion spectrum of $v' = 41$ level of $(3)^1\Sigma^+$ taken with molecules in $v'' = 91$ level of $X^1\Sigma^+$. The spectrum gives rotational constants of both ground and excited states. In addition, the width of the spectrum enables us to estimate the transition strength.

Fig. 2 shows a depletion spectrum for the $v' = 41$ level of the $(3)^1\Sigma^+$ state, which was used as an intermediate state for the STIRAP transfer from the $v'' = 91$, $J'' = 0$ level of $X^1\Sigma^+$ to the $v'' = 0$, $J'' = 0$ level [18]. We can extract transition strengths as well as rotational constants for both ground and excited states from the spectra. In the appendix, we show that an approximate representation of the full-width-half-maximum (FWHM) of a depletion spectrum is given by

$$2\Delta \sim 0.79\Omega\sqrt{\Gamma\tau}. \quad (1)$$

where Ω is the Rabi frequency; Γ, the natural width of the excited state; and τ, the duration of spectroscopy. Roughly speaking, the width increases not only with the light intensity but also with the duration of spectroscopy. In our case, the duration was estimated as a few milliseconds on the basis of the temperature of the molecules and beam diameter of the depletion laser. The natural width of the $(3)^1\Sigma^+$ state was not precisely known, but it was obtained as $2\pi \times 300$ kHz from an ab initio calculation [20]. In the following discussion, we derive the Rabi frequency from the observed spectrum by assuming τ as 2 ms, Γ as $2\pi \times 300$ kHz, and $\sqrt{\Gamma\tau}$ as 60.

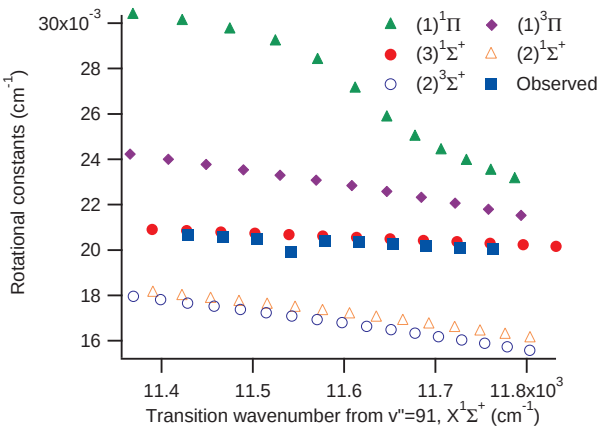

FIG. 3. Comparison between calculated and observed rotational constants. Calculated rotational constants of five molecular states in this range are plotted against energy levels from the ground atomic threshold. The observed rotational constants are in good agreement with those obtained from the *ab initio* potential of the $(3)^1\Sigma^+$ state. There is a systematic deviation of ∼1% between the observed values and *ab initio* values, which indicates the inaccuracy of the *ab initio* potential.

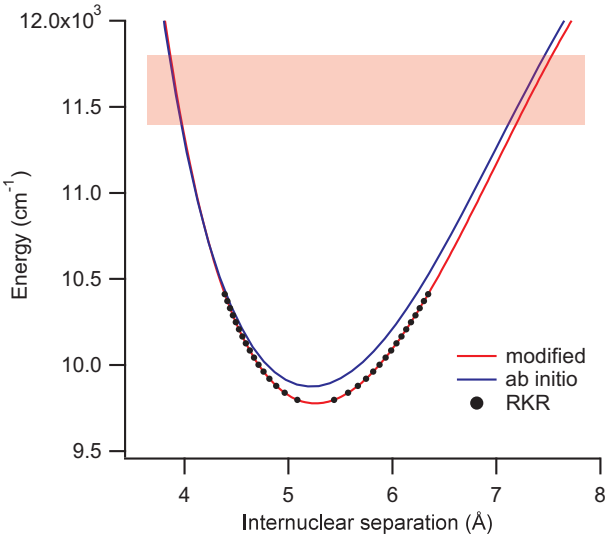

FIG. 4. Potential energy curves of $(3)^1\Sigma^+$ state. The modified potential obtained in the present study is compared with the *ab initio* potential and the experimental RKR potential. The shaded area denotes the region where depletion spectra were obtained.

III. ANALYSIS

Although the *ab initio* potential [21] enabled us to identify the symmetry of the observed spectra without any ambiguity, it gave rotational constants that exceeded the experimental ones by approximately 1% (Fig. 3). There were two reasons for this deviation. First, the potential minimum exceeded the minimum of the RKR curve by 97 cm^{-1}. Second, the outer turning point was at the shorter internuclear separation than the RKR potential. We found that the variation in the observed transition strengths could not be understood with the *ab initio* potential. The observations could not be attributed to the small change in the vibrational quantum number, which corresponded to the energy difference in the minimum of the RKR and the *ab initio* potentials. These facts indicate that the *ab initio* potential is inaccurate. In order to obtain an accurate potential, we carried out DPF analysis, whereby a potential is iteratively modified until its eigenvalues coincide with those determined from the experimental spectra [15]. With the aid of the phiFIT program code [22], we first constructed an analytical Extended Morse Oscillator (EMO) potential of the $(3)^1\Sigma^+$ state on the basis of (1) the RKR curve, (2) a few points from the inner curve of the *ab initio* potential, and (3) a few points around 12500 cm^{-1} from the outer curve of the *ab initio* potential. The potential curve of the ground state $X^1\Sigma^+$ was also required for the calculations. We used an EMO potential fitted to an accurate, experimentally determined potential [23]. Then, the analytical potential of the $(3)^1\Sigma^+$ state was modified to reproduce our data by using the DPotFit program code [24]. A good convergence was achieved when we modified the potential significantly by manually moving the points from the *ab initio* potential. This procedure was repeated until the eigenvalues of the potential were within 0.05 cm^{-1} of the observed levels, i.e., only 0.14% of the vibrational level spacing. The remaining deviations were presumably due to the incomplete analytical function used to represent the potential. Table I lists the final potential parameters. These parameters are used to represent the potential energy curve in the following form:

$$\begin{aligned} V(R) =& V_{\min} + D_e(1 - e^{-\phi(R)(R-R_e)})^2 \\ \phi(R) =& \sum_{i=0}^{12} \phi_i y(R, R_e)^i \\ y(R, R_e) =& \frac{R^3 - R_e^3}{R^3 + R_e^3}. \end{aligned} \tag{2}$$

Fig. 4 shows the RKR potential, *ab initio* potential and modified potential. At the new potential, rotational

TABLE I. Parameters for EMO potential obtained via DPF analysis of the observed spectra. The units are cm^{-1} for V_{min} and D_e, Åfor R_e, and $Å^{-1}$ for ϕ_i.

Parameter	Value	Parameter	Value
$V_{\min}$	9777.6963	ϕ_5	-0.804673587
D_e	3246.0363	ϕ_6	3.00474008
R_e	5.25904119	ϕ_7	11.3877324
ϕ_0	0.449794066	ϕ_8	-2.140717462
ϕ_1	0.200265883	ϕ_9	-39.73110586
ϕ_2	0.406840126	ϕ_{10}	-17.01400311
ϕ_3	0.207884795	ϕ_{11}	50.93279647
ϕ_4	-0.476349301	ϕ_{12}	44.83137419

TABLE II. Comparison between observed, *ab initio*, and modified values for vibrational energies (E) and rotational constants (B). Vibrational energies are energy levels of the $J' = 1$ level. Error bars in vibrational energies are 2×10^{-3} cm^{-1}, whereas those in rotational constants are 5×10^{-5} cm^{-1}. Observed vibrational energies are reproduced within 5×10^{-2} cm^{-1}, whereas observed rotational constants are reproduced within 7×10^{-5} cm^{-1}. The vibrational numbering for *ab initio* values is deviated by 2 because the potential minimum lies below that of the correct potential.

v'	E (cm^{-1})			B (10^{-2}cm^{-1})		
	Obs.	*ab initio* - Obs.	Mod. - Obs.($\times 10^{-3}$)	Obs.	*ab initio* - Obs.($\times 10^{-2}$)	Mod. - Obs. ($\times 10^{-3}$)
41	11428.965	-1.5	2.5	2.067	1.9	-7.0
42	11466.644	-1.6	29.9	2.056	2.3	-1.7
43	11504.193	-1.8	42.6	2.05	2.4	-1.5
44	11541.484	-1.9	164.2	1.99	7.8	52.6
45	11578.919	-2.2	-11.4	2.038	2.4	-1.5
46	11616.036	-2.4	-28.0	2.037	1.8	-6.8
47	11652.982	-2.6	-37.3	2.027	2.2	-3.2
48	11689.751	-2.7	-37.5	2.017	2.5	0.3
49	11726.308	-2.7	1.2	2.008	2.9	2.5
50	11762.685	-2.7	43.0	2.005	2.5	-1.4

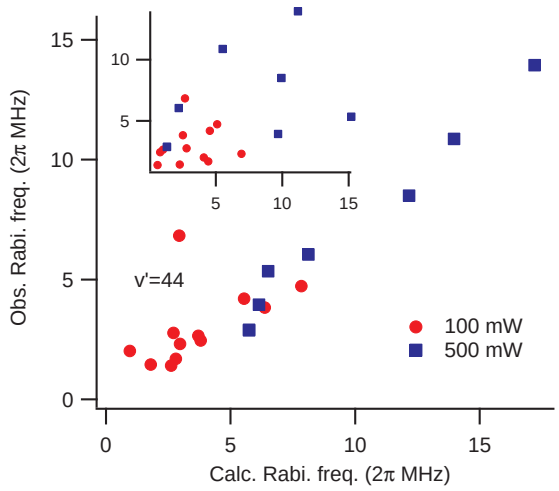

FIG. 5. Observed and calculated transition strengths. Observed values are determined from the spectra obtained via a depletion laser at 100 mW (red circle) and 500 mW (blue rectangle). Calculations based on the modified potential can explain the variation in transition strengths with respect to the vibrational levels in terms of the Franck-Condon factors. The point deviated from other points corresponds to the $v' = 44$ level, which is expected to be mixed with other states. The inset shows the same plot based on the *ab initio* potential.

constants were reproduced within 0.3% of the observed values (Table I). We excluded the $v' = 44$ level from the analysis because the characteristics of this level are anomalous; a much larger transition strength, a much smaller rotational constant, and a much larger deviation in a vibrational energy were observed at this level. These features indicate that this level was coupled to the $(2)^1\Sigma^+$ state which was observed at $\sim$1 cm^{-1} above the $v' = 44$ level.

The most important implication of this analysis is that the variation in the transition strengths with respect to the vibrational levels of the excited state can be accurately explained on the basis of the new potential. Fig. 5 shows a plot of the Rabi frequencies derived from the observed spectra against those calculated from the corrected potential. For comparison, the same plots based on the *ab initio* potential are also shown. The calculated values are calibrated on the basis of our recent measurement of the transition dipole moment between $(3)^1\Sigma^+$, $v' = 41$ and $X^1\Sigma^+$, $v'' = 91$, $0.035(2)ea_0$, determined via dark resonance spectroscopy of the rovibrational ground-state molecules. Weakly bound molecules have more than 90 nodes in their wavefunction; hence, the FCFs are highly dependent on the wavefunction of the excited state. In other words, the FCFs can serve as a sensitive measure of the accuracy of wavefunctions. Our results show that accuracies of 0.14% in vibrational level spacings and 0.3% in rotational constants are sufficient to predict the FCFs from weakly bound levels; these values are justified by considering the typical size of nodes in the radial wavefunction. On one hand, the weakly bound level $v'' = 91$ in the ground state $X^1\Sigma^+$ has an outer turning point of $\sim$10 Åand an inner turning point of $\sim$2 Åin the internuclear distance. Within these two points, there are 91 nodes; hence each node has a typical size of $\sim$0.1 Å. Therefore, the required accuracy for representing the wavefunction is $\sim 10^{-2}$ Å. On the other hand, in the present analysis, an accuracy of $\sim$0.3% in rotational constants or $\sim$0.15% in internuclear distance is obtained for the $(3)^1\Sigma^+$ state because the relation between the rotational constant B and the internuclear distance R is given by $B \propto R^{-2}$. Assuming the typical size of molecules in the v' =41–50 levels of $(3)^1\Sigma^+$ as 6 Å, we can derive the accuracy of the modified potential in the radial direction as $\sim 10^{-2}$ Å; this value is in good agreement with the required accuracy for representing the weakly bound level.

Now that we obtained an accurate potential curve as well as the absolute values of the transition dipole moment of the $v' = 41$, $(3)^1\Sigma^+$ level with the $v'' = 0$ and $v'' = 91$ levels of $X^1\Sigma^+$, we can predict the transition

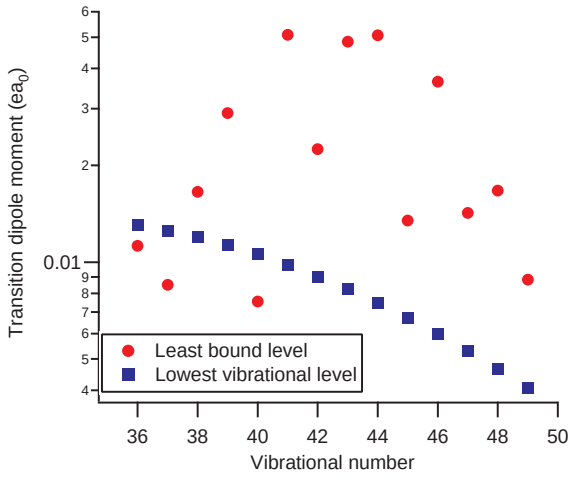

FIG. 6. Transition dipole moments of the $(3)^1\Sigma^+$ state with the $X^1\Sigma^+$ state calculated from the experimentally obtained accurate potential. The absolute values for weakly bound levels are calibrated by dark resonance spectroscopy for the transition $v' = 41, (3)^1\Sigma^+ \leftarrow v'' = 91, X^1\Sigma^+$ whereas those for the rovibrational ground state are calibrated by dark resonance spectroscopy for the transition $v' = 41, (3)^1\Sigma^+ \leftarrow v'' = 0, X^1\Sigma^+$.

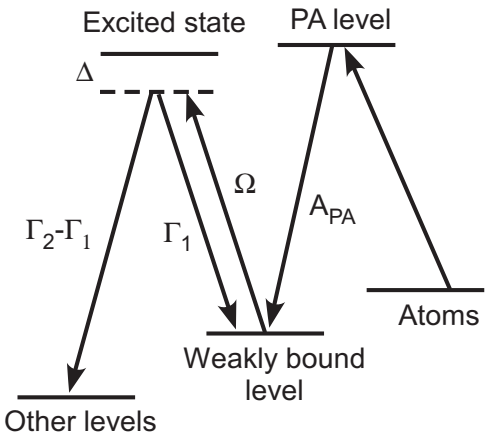

FIG. 7. Energy levels relevant to depletion spectroscopy of photoassociated molecules. Weakly bound molecules are formed at a rate of $A_{\rm PA}$. A laser having Rabi frequency of Ω detuned from the resonance by Δ excites ground state molecules. Excited molecules spontaneously decay to the initial level and other levels at rates of Γ_1 and $\Gamma_2 - \Gamma_1$, respectively. We mainly consider a situation where $\Gamma_2 > \Gamma_1$ is satisfied.

dipole moment for each transition. Fig. 6 shows our prediction for the transition dipole moments of the $(3)^1\Sigma^+$ state with the least bound state and for those with the lowest rovibrational level ($v'' = 0$). The $v' = 41$ level used in Ref. 18 has favorable wavefunction overlaps with both the weakly bound and the lowest rovibrational levels; however other levels such as $v' = 38$ and $v' = 39$ can potentially serve as an intermediate state for the STIRAP transfer of weakly bound molecules to the rovibrational ground state. The potential presented herein can enable an accurate prediction for other isotopic combinations of KRb. Further, the present method for achieving an accurate potential and verifying its accuracy can be extended to other molecular states that exhibit significant spin-orbit mixing by evaluating eigenvalues via coupled channel calculations including spin-orbit interaction.

IV. CONCLUSION

The $(3)^1\Sigma^+$ state of KRb was investigated via the depletion spectroscopy of ultracold molecules formed by the photoassociation of laser-cooled ^{41}K and ^{87}Rb atoms. The spin-orbit mixing of other electronic states with the $(3)^1\Sigma^+$ state was negligible; hence, we could assume this state as a single potential. The simplicity of the $(3)^1\Sigma^+$ state enabled us to modify the potential to reproduce our observations as well as to assign the spectra. We observed 10 vibrational levels in the range 11400–11800 cm^{-1} with respect to the ground atomic threshold. We developed a theoretical model that related the spectral width with the Rabi frequency, which was used to compare the transition strengths for each vibrational level. Rotational constants extracted from the observed spectra showed a 1% deviation from those calculated using an *ab initio* potential. By carrying out DPF analysis, we constructed an accurate potential that reproduced energy levels with an accuracy of 0.14% in vibrational level spacing and 0.3% in rotational constants. The variation in transition strengths among vibrational levels could be understood in terms of FCFs calculated with the modified potential. Our results indicate that the transition strengths from weakly bound levels serve as a sensitive measure of wavefunctions, which can be used to test the accuracy of the potential curve. In general, the proposed procedure can be adopted for constructing an accurate potential and verifying its accuracy on the basis of rotational spectra for weakly bound molecules.

Appendix: Analytical expression for the line shape of a depletion spectrum

We consider a general situation, as shown in Fig. 7, and we assume that radiative transitions occur much faster than the time variation of the population in each molecular level because of the photoassociative creation of molecules. We first consider the evolution of the population in the ground and excited states of a single molecule. The optical Bloch equation for this system can be written

as

$$\begin{aligned}\frac{ds}{dt} =&-(\Gamma_2-\Gamma_1)\frac{s-w}{2}\\ \frac{dw}{dt} =&(\Gamma_2+\Gamma_1)\frac{s-w}{2}-2\Omega\mathrm{Im}(\widetilde{\rho_{eg}})\\ \frac{\widetilde{\rho_{eg}}}{dt} =&-(\frac{\Gamma_2}{2}-i\Delta)\widetilde{\rho_{eg}}+\frac{i}{2}w\Omega\end{aligned} \tag{A.1}$$

where $s=\rho_{gg}+\rho_{ee}$, $w=\rho_{gg}-\rho_{ee}$, and $|e>$ and $|g>$ denote an excited state and a weakly bound level, respectively. Δ and Ω denote the detuning frequency and the Rabi frequency, respectively. The decay rates from the excited state to the initial weakly bound level and to other levels are given by Γ_1 and Γ_2, respectively. The photoassociation rate is denoted by A_{PA}. The width is much larger than the Rabi frequency in the experiment; hence, we can assume that the time evolution of s and w is much slower than that of $\widetilde{\rho_{eg}}$. Thus, we can set $d\widetilde{\rho_{eg}}/dt=0$ and obtain the following expression for $\widetilde{\rho_{eg}}$:

$$\widetilde{\rho_{eg}}=\frac{i\Omega w}{\Gamma_2-2i\Delta} \tag{A.2}$$

Substituting Eq.(A.2) in Eqs.(A.1), we obtain alternative equations for s and w as

$$\begin{aligned}\frac{ds}{dt} =&-(\Gamma_2-\Gamma_1)\frac{s-w}{2}\\ \frac{dw}{dt} =&(\Gamma_2+\Gamma_1)\frac{s-w}{2}-\frac{2\Omega^2\Gamma_2 w}{\Gamma_2^2+4\Delta^2}\end{aligned} \tag{A.3}$$

Here, we assume that the time taken by the mean value of the population ratio w/s to attain a constant value z after is greater than the typical time for radiative transitions. By using the relation $w=zs$, Eqs.(A.3) give following equations:

$$\begin{aligned}\frac{ds}{dt} =&-(\Gamma_2-\Gamma_1)\frac{1-z}{2}s\\ z\frac{ds}{dt} =&(\Gamma_2+\Gamma_1)\frac{1-z}{2}s-\frac{2\Omega^2\Gamma_2}{\Gamma_2^2+4\Delta^2}zs\end{aligned} \tag{A.4}$$

Substituting the first equation in the second equation, we obtain a time-independent equation for z:

$$(1-z)\left[\Gamma_2(1+z)+\Gamma_1(1-z)\right]=\frac{4\Omega^2\Gamma_2}{\Gamma_2^2+4\Delta^2}z \tag{A.5}$$

This equation is readily solved, and it gives the following expression for z.

$$\begin{aligned}z=&\frac{\sqrt{(1+k^2)\Gamma_2^2+2\Gamma_1\Gamma_2 k}-(k\Gamma_2+\Gamma_1)}{\Gamma_2-\Gamma_1}\\ k=&\frac{2\Omega^2}{\Gamma_2^2+4\Delta^2}\end{aligned} \tag{A.6}$$

This expression is used in the following discussion. Next, we derive rate equations for the population in the ground and excited molecular levels for the number of molecules:

$$\begin{aligned}\frac{dN}{dt} =&A_{\mathrm{PA}}-(\Gamma_2-\Gamma_1)N_e\\ N_e=&\frac{1-z}{2}N\\ N_g=&\frac{1+z}{2}N\end{aligned} \tag{A.7}$$

where N_g and N_e denote the number of molecules in the ground and excited states, respectively, and $N=N_g+N_e$ is the total number of molecules. In these rate equations, a typical timescale is of the order of 1 ms, and it is governed by A_{PA}. This is much longer than the typical timescale for radiative transitions in most cases ($\leq$1 μs). The time evolution of N_g is given by

$$\frac{dN_g}{dt}=\frac{1+z}{2}A_{\mathrm{PA}}-\frac{1-z}{2}(\Gamma_2-\Gamma_1)N_g \tag{A.8}$$

Thus, the solution for N_g is given by

$$\begin{aligned}N_g(\tau)=&\frac{A_{\mathrm{PA}}}{\Gamma_2-\Gamma_1}\frac{1+z}{1-z}\\ &\times\left(1-\exp\left[-\frac{1-z}{2}(\Gamma_2-\Gamma_1)\tau\right]\right).\end{aligned} \tag{A.9}$$

This expression gives the line shape of a depletion spectrum for a duration τ. Assuming $(\Gamma_2-\Gamma_1)\tau\gg 1$, Eq.(A.9) gives

$$N_g(\tau)\to\frac{A_{\mathrm{PA}}}{\Gamma_2-\Gamma_1} \tag{A.10}$$

on resonance ($\Delta=0$ and $w\to 0$), whereas N_g at an infinite detuning ($\Delta\to\infty$ and $w\to 1$) is given as

$$N_g(\tau)\to A_{\mathrm{PA}}\tau \tag{A.11}$$

N_g at an infinite detuning is much larger than N_g on resonance. Thus, the width of the spectrum is determined by finding w such that it satisfies

$$N_g(\tau)=\frac{1}{2}A_{\mathrm{PA}}\tau. \tag{A.12}$$

Substituting Eq.(A.9) in Eq.(A.12) and rewriting the equation with a new variable $x\equiv 1-z(\ll 1)$, we obtain the following equation:

$$\frac{2}{x}\left(1-\exp\left[-\frac{x}{2}(\Gamma_2-\Gamma_1)\tau\right]\right)=\frac{\Gamma_2-\Gamma_1}{2}\tau \tag{A.13}$$

A rigorous solution of this equation is given by

$$\begin{aligned}x=&\frac{4+2\mathrm{W}(-2/e^2)}{(\Gamma_2-\Gamma_1)\tau}\\ =&\frac{1}{(\Gamma_2-\Gamma_1)\tau}\times 3.18724...\end{aligned} \tag{A.14}$$

where W is the Lambert W function. Thus, the parameter k in Eqs.(A.6) is given by

$$k = \frac{3.18724(1 - 1.59362/\Gamma_2\tau)}{(\Gamma_2 - \Gamma_1)\tau - 3.18724} \tag{A.15}$$

Assuming $(\Gamma_2 - \Gamma_1)\tau \gg 1$, we obtain the following expression for FWHM:

$$2\Delta \approx 0.79\Omega\sqrt{(\Gamma_2 - \Gamma_1)\tau} \tag{A.16}$$

When decays from the excited state to the initial state are negligible ($\Gamma_2 \gg \Gamma_1$), we obtain a simple relation (1). It is difficult to evaluate the numerical factor $\sqrt{\Gamma\tau}$ precisely; therefore, the width of a depletion spectrum cannot serve as an accurate measure of the transition strength. However, the expression (1) enables us to systematically compare transition strengths for different vibrational levels.

ACKNOWLEDGMENTS

We thank P. Naidon and T. Kishimoto for insightful discussions, and K. Oasa, Y. Tanooka, and K. Mori for their assistance with the experiment. K. A. and D. A. acknowledge the support of the Japan Society for the Promotion of Science.

[1] R. V. Krems, W. C. Stwalley, and B. Friedrich, *Cold molecules: theory, experiment, applications* (CRC, Boca Raton, 2009).
[2] L. D. Carr, D. DeMille, R. V. Krems, and J. Ye, New J. Phys. **11**, 055049 (2009).
[3] K. M. Jones, E. Tiesinga, P. D. Lett, and P. S. Julienne, Rev. Mod. Phys. **78**, 483 (2006).
[4] T. Kohler, K. Goral, and P. S. Julienne, Rev. Mod. Phys. **78**, 1311 (2006).
[5] J. M. Sage, S. Sainis, T. Bergeman, and D. DeMille, Phys. Rev. Lett. **94**, 203001 (2005).
[6] M. Viteau *et al.*, Science **321**, 232 (2008).
[7] J. Deiglmayr *et al.*, Phys. Rev. Lett. **101**, 133004 (2008).
[8] K.-K. Ni *et al.*, Science **322**, 231 (2008).
[9] F. Lang *et al.*, Phys. Rev. Lett. **101**, 133005 (2008).
[10] J. G. Danzl *et al.*, Nat. Phys. **6**, 265 (2010).
[11] K. Bergmann, H. Theuer, and B. W. Shore, Rev. Mod. Phys. **70**, 1003 (1998).
[12] N. V. Vitanov, M. Fleischhauer, B. W. Shore, and K. Bergmann, Adv. At. Mol. Opt. Phys. **46**, 55 (2001).
[13] P. Kral, I. Thanopulos, and M. Shapiro, Rev. Mod. Phys. **79**, 53 (2007).
[14] G. Herzberg, *Molecular spectra and molecular structure. 1. Spectra of diatomic molecules* (Van Nostrand, New York, 1950).
[15] J. Seto, R. Le Roy, J. Vergès, and C. Amiot, J. Chem. Phys. **113**, 3067 (2000).
[16] D. Wang *et al.*, Phys. Rev. A **75**, 032511 (2007).
[17] C. Amiot, J. Vergès, J. d'Incan, and C. Effantin, Chem. Phys. Lett. **315**, 55 (1999); C. Amiot, *ibid.* **318**, 289 (2000).
[18] K. Aikawa *et al.*, Phys. Rev. Lett.(in press) (2010).
[19] K. Aikawa *et al.*, New J. Phys. **11**, 055035 (2009).
[20] R. Beuc *et al.*, J. Phys. B **39**, S1191 (2006).
[21] S. Rousseau, A. R. Allouche, and M. Aubert-Frecon, J. Mol. Spectrosc. **203**, 235 (2000).
[22] R. J. Le Roy, "A Computer Program to Fit Pointwise Potentials to Selected Analytic Functions," (2007), current version is betaFIT 2.0, available at http://leroy.uwaterloo.ca/programs.html.
[23] A. Pashov, O. Docenko, M. Tamanis, R. Ferber, H. Knockel, and E. Tiemann, Phys. Rev. A **76**, 22511 (2007).
[24] R. J. Le Roy, J. Y. Seto, and Y. Huang, "A Computer Program for Fitting Diatomic Molecule Spectral Data to Potential Energy Functions," (2006), available at http://leroy.uwaterloo.ca/programs.html.